Bio-Internet of things through micro-circulation network: A molecular communication channel modeling

Guodong Yue, *Graduate Student Member, IEEE,* Qiang Liu, *Senior Member, IEEE,* Kun Yang, *Fellow, IEEE,*

***Abstract*—The future of the Internet of Things (IoT) holds great promise, particularly in the realm of healthcare, where the concept of Bio-Internet of Things (B-IoT) has gained significant attention. B-IoT involves the coordination of monitoring and treatment within the human body using bio-implants that require communication. However, how to efficiently communicate among bio-implants is seldom studied. Molecular communication (MC), which uses molecules as information carriers, is a novel communication method of nano-devices for its excellent biocompatibility and low energy consumption. In every part of the body, there is a micro-circulation network (MCN) responsible for substance exchange which can be utilized as a channel to deliver information efficiently by Bio-implants. However, since the structure of MCN is complicated and the characteristics of blood flow vary, there is not yet a mature channel modeling on MCN, making it impossible to design and evaluate the performance of B-IoT. In this paper, we address the need for efficient communication channels in B-IoT by exploring the potential of micro-circulation networks (MCN) in MC. We have fully analyzed the characteristics of MCN and blood flow and derived the mathematical model of channel impulse response. We also built a simple end-to-end communication model based on MCN and analyzed its error probability and mutual information from a communication perspective. The numerical results have shown that MCN is an effective communication channel of MC for B-IoT in the scale of μm and mm.**

***Index Terms*—Molecular communication, Micro-circulation, channel modeling, bio-implants**

I. Introduction

In nano-medicine and healthcare, there is an envision of Bio-internet of things (B-IoT) within the human body [1]. It comprises smart bio-implants and nanomachines as nodes that can conduct certain tasks such as collecting, processing and forwarding sensor information to help coordinate body monitoring and treatment. There are already some metal or organic implants like vascular stents being used in surgery to treat diseases including atherosclerosis and aneurysm [2]-[6], however, these stents have the potential of being transformed into intelligent nodes by integrating certain smart modules. So far, there are some early realizations of biosensors. There are synthetic biosensors that can collect and process information, as discussed in [7]−[9]. Additionally, there are Lab-on-a-Chip devices at the nano-scale that enable biological tests [10][11], as well as nanomachines capable of swimming in the bloodstream to perform tasks [12][13]. Anyhow, these biosensors of B-IOT need to transmit and receive signals just like that in wireless sensor network. However, electromagnetic communication is not suitable in nano-scale for multiple reasons. First, it is very difficult to scale devices of wireless communication such as antennas in the form to micro and nano-meters [14][15]. Second, wireless signals cannot propagate well in fluids. Third, electromagnetic wave with high frequencies may cause harmful influences on human body [17]. As an alternative, Molecular communication (MC) is particularly suitable in micro-scale scenarios for its excellent bio-compatibility and low-energy consumption [18]. It is very significant to explore the potential of MC to meet the communication needs of future B-IoT applications.

Molecular communication (MC) is a novel communication technology which uses molecules as information carriers [16]. Like any communication paradigm, MC system involves transmitters, communication channel and receivers [19]-[21]. The transmitters and receivers are nanomachines or bio-implants, which are made of nano-material or gene-edited cells and bacteria [22]. The communication channel is usually assumed to be in a liquid environment, like body fluid and blood. There are multiple modulation techniques in MC, for example, the transmitted information can be modulated in the concentration, type, time of release and possibly other properties of the emitted molecules [23]. Nanonetwork is a promising application of molecular communication [25]-[29]. The delivery of information requires molecule transfer in the environment and the communication channel determines how the information molecules move from transmitter to receiver. So far, diffusion based channels have been the most studied molecular communication channels since the released molecules can passively diffuse to the destination without extra energy supply, and are received and measured by the receiver [31]-[33]. However, due to the randomness of Brownian motion, some information molecules have to take a longer time to arrive at the receiver which means these molecules may arrive at the receiver in later time slots and cause inter-symbol interference (ISI), especially in long distances [34]. ISI

This work was supported in part by the National Natural Science Foundation of China under Grant 62071101, and the Municipal Government of Quzhou under Grant No. 2023D008. (*Corresponding author: Qiang Liu.*)

Guodong Yue is with School of Information and Communication Engineering, University of Electronic Science and Technology of China, Chengdu 611731, China (email: 202211012429@std.uestc.edu.cn).

Qiang Liu is with the Yangtze Delta Region Institute (Quzhou), University of Electronic Science and Technology of China, Quzhou, Zhejiang 324000, China (email: liuqiang@uestc.edu.cn).

Kun Yang is with the School of Computer Science and Electronic Engineering, University of Essex, CO4 3SQ Colchester, U.K, and also with the School of Information and Communication Engineering, University of Electronic Science and Technology of China, Chengdu 611731, China (e-mail: kunyang@essex.ac.uk).

is an important problem of a diffusion based communication system and is known to deteriorate the error performance for higher data rates [35]. In order to achieve higher data rates while maintaining a sufficiently low error performance, and to extend the effective communication distance, it is important to find alternatives other than diffusion based channel. One of the alternatives is flow-based channel. Fluid flow is thought to be faster and more reliable. In previous literature, the flow is often simply introduced to an unbounded diffusion scenario, making it simply a biased diffusion[36] and the diffusion still dominates. Therefore, it is more important to turn to bounded fluid channel[37], for example, the blood vessel. Blood vessels are responsible for transportation of nutrition and oxygen, making it a natural "high-way" in body [38]. In addition, the group of molecules within the blood vessel are transported by blood flow and confined by the blood vessel wall, which means they are fast and perfectly directed and will not diffuse everywhere. The properties of blood vessels and flow can guarantee reliable molecule transportation even in a long range, and avoid the shortcomings of diffusion based channel. According to fluid mechanics, the blood flow in most vessels belongs to laminar flow [32], which makes the analysis easier, for the turbulent flow is way more complicated. The blood vessel in the body consists of three parts, the artery, the capillary and the vein. The bloodstream goes first to the arteries, then to the capillaries and finally to the veins, and back to the heart, completing a cycle, which is the process of systemic circulation. Within each tissue, there are smaller systemic circulations, called micro-circulations[39], made up of arterioles, capillaries, and venules.

Since a lot of medic-scenarios focus on individual tissue, it is important to build a communication model based on micro-circulations.

In this paper, we have analyzed the characteristics of blood vessel and blood flow and based on the physical model of micro-circulation, the shunt and convergence of blood, and the corresponding velocity changes are analyzed. We built a molecular communication channel model based on micro-circulation and obtained its channel impulse response (CIR). The performance of communication is evaluated and demonstrated by both theoretical derivation and simulation. The main contributions of this paper are listed as follows:

1) We proposed a communication system based on micro-circulation network, which can help transmit signals in a long range.
2) The characteristics of every part of the communication system are mathematically modeled.
3) The BER and Channel Capacity of the entire system are evaluated and discussed from the perspective of communication.

II. Preliminaries

This section will introduce the bio-internet of things (B-IoT), molecular communication (MC) and micro-circulation which includes arteriole, capillary network and venule, respectively.

A. Bio-Internet of things

The bio-internet of things is an envision that promises to revolutionize medicine and healthcare in society [1]. By harnessing the capabilities of biological cells within the bio-chemical realm, B-IoT offers a transformative pathway for a range of applications. These include intra-body sensing and actuation networks, as well as the ability to effectively monitor and mitigate the impact of toxic agents and pollution on the environment. The basis of B-IoT is the communication and interaction of Bio-implants and nanomachines derived from engineered biological cells. The natural environment serves as the main inspiration for studying communication techniques such as molecular communication. Some literature have proposed health monitoring molecular networks based on B-IoT. [30][61], where bio-implants are stationary bio-sensors mounted at certain critical locations within blood vessels to collect and forward bio-information like important blood routine indicators, such as blood lipids, uric acid, etc. Fig. 1 shows a possible B-IoT scenario in which the data of three nodes on the branches will be transferred to the sink node in the form of information molecules through blood vessels[30]. Just like Wireless Sensor Network (WSN), it is divided into different clusters responsible for monitoring different parts of the human body. Each cluster is composed of multiple sub-sensors and a main-sensor as the cluster head. The sub-sensor can collect the bio-information and forward it to the main-sensor. The main-sensor is integrated with a wireless communication module and can send information to outside user-end such as cellphones. A key challenge to realizing such a network is to guarantee that each sub-sensor can smoothly use bloodstream to transmit information. Since blood vessel network is a complicated flow-based channel, it is very important to study its properties and conduct modeling on it before utilizing it as a communication channel.

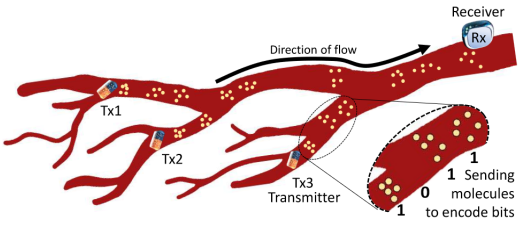

Fig. 1: Bio-internet of things [30]

B. Molecular Communication

From a communication perspective, molecular communication emerges as novel communication method driven by emerging technologies such as nanotechnology. Scientists aspire to interconnect these nano-devices through information exchange, forming nano-networks, to accomplish intricate tasks in small-scale environments. Compared to electromagnetic communication, MC systems deployed in small-scale environments are not limited by the size of the transceiver devices.

Currently, the entities of molecular communication which are called bio-implants and nanomachines, are primarily de-

signed and implemented using nano-material based or bio-inspired approaches. The transmitter is to encode and modulate information while generating and releasing information molecules. In the fluid channel, the released molecules will reach the receiver by diffusion and advection. The receiver's task is to sense and demodulate the output of the channel, extracting the information carried by the information molecules.

There are multiple modulation techniques in MC system. Information can be modulated in the concentration, type and timing of molecules[68]. Concentration Shift Keying (CSK) is the typical binary modulation technique in molecular communication realm. It is similar to ASK(Amplitude Shift Keying) in electromagnetic communication. It uses the concentration of received molecules as the amplitude of signal. In each time slot, the transmitter releases a certain number of molecules to indicate '1' and releases nothing to indicate '0'. At the receiver, if the received number of molecules exceeds the threshold, the receiver will demodulate it as "1", otherwise as "0".

Overall, compared to electromagnetic communication, MC offers deployment advantages in micro-scale environments. Moreover, the information carriers have the potential for interaction with cells or tissues within the biological body, making it more bio-compatible. Therefore, MC holds great potential in constructing intra-body communication systems and has vast applications in fields such as disease diagnosis and treatment[46]–[48], drug delivery[49]–[52], and the establishment of artificial immune systems[54].

C. Micro circulation network

In organisms, the circulatory system can be divided into overall level, organ level and organization level according to its scale and function. The main function of the circulatory system at the whole level and organ level is to transport fluid to tissues that need oxygen and nutrients, while the micro-circulation system at the tissue level is mainly involved in functional physiological activities such as metabolism and material exchange. The number of micro-circulatory vessels is rich, and the vessel wall is thin, which is an important place for material exchange between blood and tissue fluid. The model of micro-circulation vascular network usually assumes that the blood vessel is a rigid cylinder, and the blood flow is a stable fluid, which is solved by Poiseuille's law.

In molecular communication, fluid based channel is far more efficient than diffusion channel, since the flow is directional and fast, reducing the loss of molecules and guaranteeing the reliability[17][37]. The MCNs in the body is inter-connected, allowing information molecules to move from one point to another through blood vessels rapidly[39]. There are already literature studying the possibility of using vascular network for molecular communication in human body for possible applications such as drug delivery[51]–[53] and disease detection[61].

Micro-circulation network is composed of arteriole, capillary networks, and venule, and can be abstracted as a layered model [55], as shown in Fig. 2. The blood first goes to arteriole, then distribute into capillary networks and eventually converges at the venule. The structure of MCN consists of

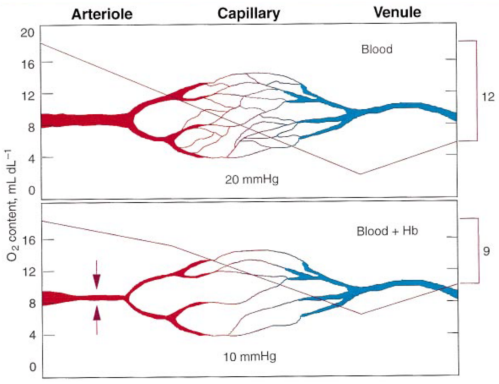

Fig. 2: Model of MCNs [55]

bifurcation and junction of blood vessels, which leads to the divergence and convergence of blood flow. Fig. 3 shows how blood flows during bifurcation and junction.

Since the blood is incompressible, the density is assumed a constant and the mass of blood is proportional to the volume of blood. The volume of blood is equivalent to the volume flow rate. By the law of conservation of matter, the blood volume flow rate should not change after bifurcation or junction as (1) shows.

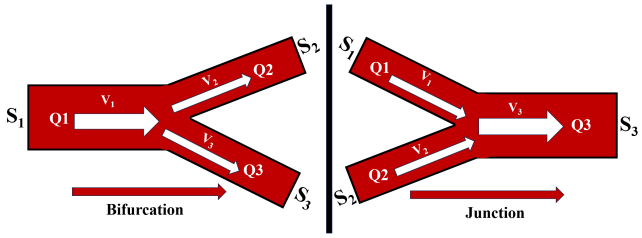

Fig. 3: Bifurcation and Junction

$$\begin{aligned} Q_1 &= Q_2 + Q_3, \\ Q_1 + Q_2 &= Q_3, \end{aligned} \tag{1}$$

where Q is the volume flow rate.

According to Continuity equation, in bifurcation

$$\begin{aligned} M_1 &= v_1 S_1 \rho, \\ M_2 &= v_2 S_2 \rho, \\ M_3 &= v_3 S_3 \rho, \\ M_1 &= M_2 + M_3, \end{aligned} \tag{2}$$

where M is the flow mass, v is the average velocity, S is the cross sectional area and ρ is liquid density. Since ρ is the same, we can rearrange the formula as

$$v_1 S_1 = v_2 S_2 + v_3 S_3. \tag{3}$$

1) Arteriole: The main function of arteriole is to transport blood and regulate flow rate. The diameter of arterioles is regulated by vascular tension and can undergo significant changes with changes in physiological environment. Therefore, arterioles can play a role in regulating MCN blood supply. The average radius of arteriole of lab rat is 90-120 μm [56], while that of pig heart is 80-100 μm[57].

2) Capillary Network: Capillaries are mainly responsible for the exchange of substances between blood and tissues. Its structure is a monolayer of endothelial cells, surrounded by a basement membrane on the outside. The diameter of capillaries is similar to the diameter of red blood cells in the stress free state of the same animal. The average inner diameter of myocardial capillaries in dogs is 5.5μm (red blood cell diameter 7.1 μm) [58], while the average inner diameter of mesenteric capillaries in rats is 11μm (red blood cell diameter 6.8 μm) [59].

3) Venule: Venule transports blood back to the large veins, ultimately returning to the heart. Its vascular wall structure is similar to that of capillaries. However, its radius is 50-60% larger than that of arteriole [60]. Due to the conservation of flow rate, the blood flow velocity at the venule is significantly lower than that at the arteriole, as the diameter of the same grade Microveins is larger than that of the arteriole. As the secondary blood vessels of capillaries, micro-vessels play a role in maintaining capillary blood pressure levels to ensure normal metabolic activity.

D. Blood flow Characteristics

Blood flow is the carrier of information molecules. We need to analyze its physical properties to find out how molecules are transported and distributed in the blood vessel.

1) Raynor number: In particular, when the variations in the flow velocity, over space and/or time, are stochastic, e.g., due to rough surfaces and high flow velocities [40], we refer to the flow as turbulent. If the flow is not turbulent, it is referred to as laminar. As a special fluid, blood contains various components such as blood cells and colloidal substances and is not an ideal fluid. It is important to determine if blood flow is laminar flow or not. In fluid mechanics, Raynor number is a dimensionless number, used as a criterion for determining if flow in a bounded environment is laminar or turbulent and is given as follows

$$Re = \frac{\rho \cdot v \cdot d}{\mu}, \tag{4}$$

where ρ is the density of fluid, v is average velocity, d is the diameter of the bounded pipe and μ is the kinematic viscosity of the fluid. Normally, the kinematic viscosity of blood is 0.0035. Normally, blood is considered as a Newtonian fluid.

For example, for flow in a straight pipe with a circular cross section of diameter d, the flow can be assumed to be laminar and turbulent for Re < 2100 and Re > 2100, respectively. For microfluidic settings, typically, Re < 10, and hence, laminar flow can be assumed. For most blood vessels, Re < 500 holds, and hence, the blood flow is typically laminar. Only in large arteries such as the aorta (the largest artery in the human body), the Reynolds number can be in the range [3400, 4500], and thereby, blood flow exhibits turbulent behavior [41][42]. Luckily, in micro-circulation, it is safe to assume the blood is laminar flow.

2) Poiseuille Flow: In the 19th century, Poiseuille described the relationship between the flow rate Q, pressure difference at both ends of the pipe ΔP, and flow resistance R of an incompressible viscous fluid flowing laminar in a cylindrical pipeline. The blood flow is also a Poiseuille flow and follows Poiseuille Law. Until now, it is the fundamental of steady blood flow theory [42]. The flow rate can be described by the following formula

$$Q = \frac{\pi r^4 \Delta P}{8\mu L}, \tag{5}$$

where r is the radius of circular cross section, L is length of the pipeline, and μ is fluid viscosity.

According to Poiseuille law, when pressure difference ΔP, length L and fluid viscosity μ are fixed, the flow rate Q is determined by the radius of circular cross section r, as illustrated in Fig. 4. It shows that

$$\frac{Q_1}{Q_2} = (\frac{r_1}{r_2})^4. \tag{6}$$

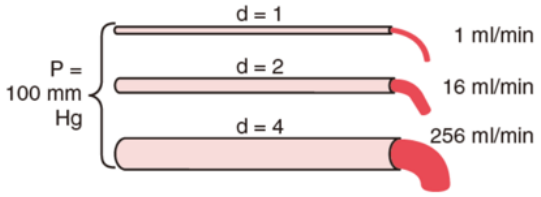

Fig. 4: Different flow rate

By combining (5) and Navier-Stokes equation, we can get the velocity profile of Poiseuille flow

$$v(r) = \frac{1}{4\mu}\frac{\Delta P}{L}(R^2 - r^2), \tag{7}$$

where $v(r)$ is the velocity profile, L is the length of the pipe, R is the radius of the vessel and r is the distance from the longitudinal axis of the vessel.

By rearranging (7), we can substitute v_m for ΔP and obtain a more straightforward formula

$$v(r) = 2v_m \cdot (1 - (\frac{r}{R})^2), \tag{8}$$

where v_m is the average velocity of the flow. We can see that velocity reaches the maximum at the center of the pipe and decreases as it approaches to the pipe wall (when $r = R$, the velocity is 0; when $r = 0$, the velocity is $2v_m$.). The distribution of velocity is shown in Fig. 5.

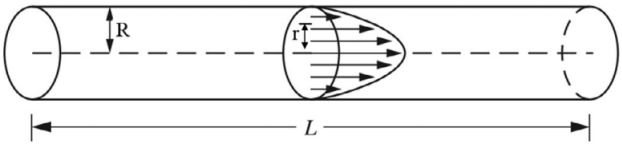

Fig. 5: Poiseuille Flow [6]

3) Peclet number: There is an important dimensionless parameter named Peclet number that weighs the influence of diffusion and flow [32]. The Peclet number, denoted by Pe, is given in (9)

$$Pe = \frac{d^2/D}{d/v_m} = \frac{v_m \cdot d}{D}, \tag{9}$$

where d is the distance to be traveled, D is the diffusion coefficient and v_m is the mean velocity of flow. If $Pe << 1$ holds, diffusion dominates flow and the spreading of molecules is almost isotropic despite a weak biased transport in the direction of the flow. On the other hand, if $Pe >> 1$ holds, flow dominates and is the major cause of the transportation of molecules and diffusion can be ignored.

Since we are focused on human body, it is important to calculate the Pe of human blood vessel. According to literature, the D of human bloodstream is $1.3 \pm 0.18 \mu m^2/ms$ [43], v_m of blood in capillary is about $1.2 \pm 0.1 mm/s$ [44] and the average length of capillary is $0.1cm$ [45]. It is calculated that Pe is about 9230 in human capillary. This result shows that in human blood vessel, flow is the major cause of transport of molecules and it is safe to ignore the effect of diffusion. Since the average velocity and length of arteriole and venule are greater than that of capillary, this conclusion holds in arteriole, venule and the entire MCN and will guide us derive the channel response of MCN in the next section.

III. System Model and Performance Evaluation

This section will introduce a communication model with a MCN as the communication channel. The molecule receiving ratio and channel impulse responses (CIR) of arteriole, capillary, venule and MCN are analyzed and derived respectively.

During the communication, CSK(Concentration Shift Keying) is chosen to be the modulation technique and bit error rate (BER) and channel capacity (C_{max}) are analyzed to evaluate its performance.

A. System Model

The overview of MCN communication channel model is given in Fig. 6. There is a transmitter implanted in the arteriole with a distance d_1 to the capillary and a receiver implanted in the venule with a distance d_3 from the capillary. The transmitter and receiver are assumed to be perfectly synchronized and the information molecules are released uniformly at every time slot with a number of N_{tx}.

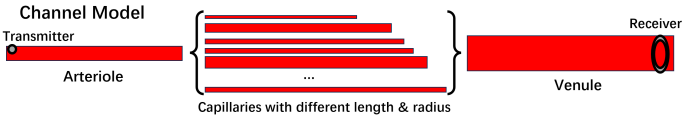

Fig. 6: MCN Channel Model

1) Blood Flow Distribution: Suppose there are n capillaries connected to the arteriole, Q_{in} indicates the inlet from arteriole, Q_{out} indicates the outlet of venule and Q_i indicates the flow rate in the i^{th} capillary. According to the law of conservation of flow, the relationship of Q_{in}, Q_i and Q_{out} are given in (11).

$$Q_{in} = \sum_{i=1}^{n} Q_i = Q_{out}. \tag{10}$$

To find out the flow distribution in the capillary network, we need to calculate for the relationship between Q_i and Q_{in}.

According to (5), the ratio of Q_1 and $Q_i (i \neq 1)$ is given as below, where Q_1 is chosen to be a reference flow rate.

$$\frac{Q_1}{Q_i} = \frac{L_i}{L_1}(\frac{r_1}{r_i})^2, \tag{11}$$

where L is the length and r is the inner radius of the capillary.

Combining (10) and (11), we can derive the relationship of Q_1 and Q_{in}

$$Q_1 = Q_{in} \frac{r_1^4}{L_1} \frac{1}{\sum_{i=1}^{n} \frac{r_i}{L_i}}. \tag{12}$$

Since the relationship of reference flow rate Q_1 and $Q_i (i \neq 1)$ is determined in (11), we can easily get the flow rate Q_i and average velocity v_i in each capillary.

$$Q_i = Q_1 (\frac{r_n}{r_1})^4 \frac{L_1}{L_i}, \tag{13}$$

$$v_i = \frac{Q_i}{\pi r_i^2}, \tag{14}$$

2) Channel Impulse Response: Assume the transmitter and receiver are passive, ring-shaped structures with a thickness of R_{tx} and R_{rx} respectively, and are attached to the wall of venule with a radius of R as shown in Fig. 7. In the receiving process, it is worth noting that only molecules that pass through the receiver will be counted, which means the receiving ratio is directly proportional to the size of the receiver R_{rx}.

Let α indicate the receiver size factor

$$\alpha = \frac{R_{rx}}{R}. \tag{15}$$

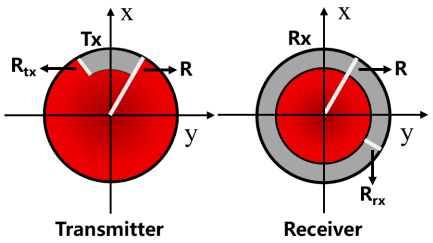

Fig. 7: Transmitter and Receiver Diagram

The derivation of h(t) is given as follows. In MC, molecules are used as the information carrier which means we need to study the motion of molecules. In the fluid environment, molecule is the subject to both diffusion and advection. The molecule distribution can be described by a time-varying spacial probability density function (P.D.F) $c(t, \mathbf{d})$, which gives a normalized concentration at time t and location $\mathbf{d}$. Assume there is a differential volume dV and the concentration within dV is $dV \cdot c(t, \mathbf{d})$. To solve for the P.D.F $c(t, \mathbf{d})$, it is necessary to solve the advection-diffusion equation which is given below:

$$\frac{\partial c(\mathbf{d}, t)}{\partial t} = D\nabla^2 c(\mathbf{d}, t) - \nabla \mathbf{v}(\mathbf{d}, t) c(\mathbf{d}, t), \tag{16}$$

where $c(\vec{d},t)$ is the concentration, D is the diffusion coefficient, ∇^2 is the Nabla operator and $\mathbf{v}$ is the velocity at $\mathbf{d}$. For a pair of given initial condition IC and boundary condition BC,

$$\begin{aligned} &\text{IC}: c(\mathbf{d}_0, t \to t_0) = N\delta(\mathbf{d}-\mathbf{d}_0) \\ &\text{BC}: c(\|\mathbf{d}\| \to \infty, t) = 0 \end{aligned} \tag{17}$$

(16) has the following solution :

$$c(\mathbf{d},t) = \frac{1}{\pi r^2}\cdot\frac{1}{\sqrt{4\pi D t}} e^{-\frac{(x-vt)^2}{4Dt}}, \tag{18}$$

where r is the radius of the blood vessel and $\frac{1}{\pi r^2}$ means a uniform cross-sectional release of molecules at the transmitter.

In our case, molecules start from the transmitter in the arteriole, passing through the artery and capillary network, and finally reaching the receiver.

By integrating (18) on the receiver volume,

$$h(\mathbf{d},t) = \int_{V_{RX}} c(\mathbf{d},t)dV_{RX}, \tag{19}$$

The molecules in the blood vessel flow forward in a uniform parabolic distribution as Fig. 5 shows, at each point of the parabolic surface, the concentration is given in (18). At the end of arteriole and capillary, there are no receivers. However, all molecules will eventually pass through them and it can be assumed that there are receivers with α=1. The velocity of molecules along the radius is determined in (8), so the time required to pass through is

$$t = \frac{d}{v(r)}. \tag{20}$$

Substitute (8) into (20) and we can get

$$t = \frac{d}{2v_m(1-\frac{r^2}{R^2})}. \tag{21}$$

As the parabola trajectory firstly hit the receiver, it must be the molecules at the center of blood vessel (r=0), the shortest time t_{min}=$d/v(0)$. As $t > t_{min}$, the passage ratio is $\frac{r}{R}$, when $\alpha = 1$. If α is not 1, when in the venule, the molecules at the hollow center will not be received, so the corresponding hollow radius $(R-R_{rx})$ needs to be subtracted, and the passage ratio becomes

$$\frac{r-(R-R_{rx})}{R}. \tag{22}$$

Therefore, we need solve for r to get the passage ratio. (21) can be rearranged to become

$$r^2 = R^2 - \frac{dR^2}{2v_m t}, \tag{23}$$

and after taking the square root of (23), and substitute (22) into it, we can get

$$h = \sqrt{1-\frac{d}{2v_m t}} - (1-\alpha), r > R - R_{rx} \tag{24}$$

The channel impulse responses of arteriole h_a, capillary h_c and venule h_v are as follows, respectively,

$$h_a(d_a,t) = \begin{cases} 0, t < t_1, \\ \sqrt{1-\frac{d_a}{2v_{in}t}}, t \geq t_1, \end{cases} \tag{25}$$

$$h_c(d_c,t) = \begin{cases} 0, t_1 < t < t_i, \\ \sqrt{1-\frac{d_c}{2v_i t}}, t \geq t_i, \end{cases} \tag{26}$$

$$h_v(d_v,t) = \begin{cases} 0, t_i < t < t_3, \\ \sqrt{1-\frac{d_v}{2v_v(t-t_i-t_1)}} - (1-\alpha), t \geq t_3 \text{ and } r > R - R_{rx} \end{cases} \tag{27}$$

The CIR of MCN with the i^{th} capillary is the product of $h_a(d_a,t)$, $h_c(d_c,t)$ and $h_v(d_v,t)$. Since there are n capillaries, the total CIR of MCN with all capillaries is obtained by summing them together, which is given in (28).

$$\begin{aligned} h(t) = \sum_{i=1}^{n} &\sqrt{(1-\frac{d_i}{2v_i(t-t_1)})(1-\frac{d_a}{2v_{in}(t-t_1)})} \\ &\cdot\left(\sqrt{1-\frac{d_v}{2v_v(t-t_1-t_i)}} - (1-\alpha)\right), \end{aligned} \tag{28}$$

where v_{in} is the mean velocity of blood flow in arteriole; d_a and d_v are the length of arteriole and venule, respectively; $t_1 = d_a/2v_{in}$ and $t_i = d_i/2v_i$ are the time that the first molecule takes to hit end of arteriole and the i^{th} capillary, respectively; d_i and v_i are the length and mean velocity of blood flow of the i^{th} capillary, respectively; v_v is the mean velocity of blood flow of venule; α is the receiver size factor. v_i is determined in

To visualize the differences between arteriole, capillary, venule, and the overall network, Fig. 8 illustrates the respective passage ratio of molecules, where the parameters are given in Table II.

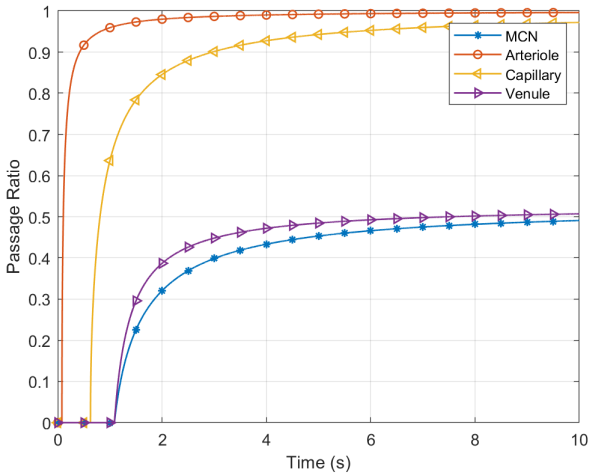

Fig. 8: Ratio of received molecules through a single capillary in MCN

B. Performance Analysis

The performance analysis includes BER and channel capacity. Assume the transmitter is a binary information source and CSK modulation [23] is utilized, which means it only sends

'1' and '0' with equal probability. To solve for the BER, it is necessary to analyze the inter-symbol interference [24].

1) Inter-Symbol Interference: The number of molecules N_r received by the receiver in a given time slot t_s is related to the number of molecules n transmitted by the transmitter, and it follows binomial distribution as

$$N_r \sim \mathcal{B}(n, p(t_s)), \tag{29}$$

where $p(t_s)$ is the probability of arrival within time slot t_s.

Since the molecules are independent and identically distributed, according to central limit theorem, when the number n is large enough and p is not close to one or zero, a binomial distribution $\mathcal{B}(n, p(ts))$ can be approximated with a Normal distribution $\mathcal{N}(np, np(1-p))$. As a result, (29) can be approximated as a Normal distribution [62][63].

$$N_r \sim \mathcal{N}(np(t_s), np(t_s)(1-p(t_s))), \tag{30}$$

where $\mathcal{N}$ is Normal Distribution.

Let N_{ISI^i} indicate the number of received molecules by the receiver at current time slot but were released i time slots before. According to [64], N_{ISI^i} is a Gaussian random variable [65] and is shown in (31).

$$\begin{aligned} N_{ISI^i} \sim & \frac{1}{2}\mathcal{N}(np((i+1)t_s), np((i+1)t_s)(1-p((i+1)t_s))) \\ & -\frac{1}{2}\mathcal{N}(np(it_s), np(it_s)(1-p(it_s))), \end{aligned} \tag{31}$$

where the factor $\frac{1}{2}$ means equal probability of transmission of bit '0' or '1'. The first term indicates the total number of molecules that are emitted at that time slot and absorbed by the receiver within all subsequent i+1 time slots and the second term indicates those molecules that were absorbed within the subsequent i time slots. Then the number of ISI molecules received by the current time slot can be expressed as

$$N_{ISI} = \sum_{i=1}^{\infty} N_{ISI^i}. \tag{32}$$

Let N_A indicate all molecules received by the receiver at current time slot and let N_C indicate molecules released by the transmitter and received by the receiver at current time slot. N_A consists two parts which are molecules from previous time slots,N_{ISI}, and from current time slot N_C. N_C is the same as (30)

$$N_A = N_C + N_{ISI}. \tag{33}$$

Let N_0 indicates the received molecule number when transmitter sends "0", while N_1 indicates the received molecule number when transmitter sends "1":

$$\begin{aligned} N_0 =& N_{ISI} \sim \mathcal{N}(\mu_0, \sigma_0^2), \\ N_1 =& N_C + N_{ISI} \sim \mathcal{N}(\mu_1, \sigma_1^2). \end{aligned} \tag{34}$$

2) Bit Error Rate Analysis: Bit error rate (BER) is an important factor to evaluate a communication model. In this model, the reason why the system generates error bit is not only because of ISI , but also because of the selection of receiver threshold. The detection of molecules by the receiver is mainly based on the comparison between the number of molecules received in the time slot and the threshold. Therefore, the selection of receiver threshold is critical to reduce the system bit error rate [66]. There is a detection method called MAP detection, which can minimize the impact of receiver threshold on bit error. Let Z denote the number of molecules observed. Then, the two detection hypotheses are:

$$\begin{aligned} H_0 : Z = \mathcal{N}_0 \sim (\mu_0, \sigma_0^2), \\ H_1 : Z = \mathcal{N}_1 \sim (\mu_1, \sigma_1^2). \end{aligned} \tag{35}$$

The MAP detection is to obtain the point estimation of the quantity that is difficult to observe based on empirical data. Similar to the MLE, the MAP incorporates the prior distribution of the quantity to be estimated. Therefore, the MAP can be regarded as the regularized MLE. Applying MAP, the formula can be derived as follows:

$$\begin{aligned} \frac{P(H_0 \mid Z)}{P(H_1 \mid Z)} &= \frac{P(H_0)\, P(Z \mid P_0)}{P(H_1)\, P(Z \mid P_1)} \\ &= \frac{\sigma_1^2}{\sigma_0^2} \exp\left\{ \frac{(Z-\mu_1)^2}{2\sigma_1^2} - \frac{(Z-\mu_0)^2}{2\sigma_0^2} \right\}. \end{aligned} \tag{36}$$

By taking logarithm and setting it to zero, the optimal decision threshold τ becomes:

$$\tau = \frac{-B + \sqrt{B^2 - 4AC}}{2A}, \tag{37}$$

where

$$\begin{aligned} A &= -\frac{1}{2}\left(\frac{1}{\sigma_1^2} - \frac{1}{\sigma_0^2}\right), \\ B &= \frac{\mu_1}{\sigma_1^2} - \frac{\mu_0}{\sigma_0^2}, \\ C &= \ln\left(\frac{\sigma_0}{\sigma_1}\right) - \frac{1}{2}\left(\frac{\mu_1^2}{\sigma_1^2} - \frac{\mu_0^2}{\sigma_0^2}\right). \end{aligned} \tag{38}$$

The BER formula can be written as

$$\begin{aligned} P_e &= \frac{1}{2}(p(1|0) + p(0|1)) \\ &= \frac{1}{2}\left(p\left(N_0 > \tau\right) + p\left(N_1 < \tau\right)\right) \\ &= \frac{1}{2}\left(Q\left(\frac{\tau - \mu_0}{\sigma_0}\right) + 1 - Q\left(\frac{\tau - \mu_1}{\sigma_1}\right)\right). \end{aligned} \tag{39}$$

3) Channel Capacity Analysis: Channel capacity is the maximum amount of information that can be transmitted per second or per symbol. The unit of information is bit. To obtain the channel capacity, we need to solve for the maximum mutual information between the transmitter and receiver.

The definition of mutual information $I(X;Y)$ is as follows

$$I(X;Y) = I(Y;X) = H(X) - H(X|Y) = H(Y) - H(Y|X), \tag{40}$$

where $H(\cdot)$ is the entropy and $H(\cdot|\cdot)$ is the conditional entropy.

The maximum of mutual information is the channel capacity

$$C = maxI(X;Y) = maxI(Y;X) = max[H(Y) - H(Y|X)]. \tag{41}$$

Assume that the source symbols are $a_i(i = 1, 2, 3...)$and the received symbols are $b_j(j = 1, 2, 3...)$. Since X it is a binary information source, there are in total two symbols, a_1 and a_2, being transmitted, and the received symbols are b_1 and b_2.

Assume that the probability that X sends a_1 is p_1 and the probability of sending a_2 is $p_2 = 1 - p_1$, the source entropy $H(X)$ is given as follows:

$$H(X) = -(p_1 \log_2 p_1 + p_2 \log_2 p_2). \tag{42}$$

The binary channel can be described by a channel transfer matrix.

TABLE I: Channel transfer matrix

Symbol	b_1	b_2
a_1	$p(b_1\|a_1)$	$p(b_2\|a_1)$
a_2	$p(b_1\|a_2)$	$p(b_2\|a_2)$

Assume that $p(b_1|a_1) = p$ and $p(b_2|a_2) = q$, and the transition matrix becomes:

Symbol	b_1	b_2
a_1	p	$1-p$
a_2	$1-q$	q

In previous part, we have given the error decision probability of $p(N_0 > \tau)$ and $p(N_1 < \tau)$, which are equivalent to $p(b_2|a_1) = 1 - p$ and $p(b_1|a_2) = 1 - q$.

To obtain the maximum of $I(Y;X)$, we need to find $H(Y|X)$ first.

$$\begin{aligned} H(Y|X) &= -\sum_{j=1}^{2}\sum_{i=1}^{2} p(a_i b_j) \log_2 p(b_j|a_i) \\ &= -[p(a_1b_1)log_2 p + p(a_1b_2)log_2(1-p) \\ &\quad + p(a_2b_1)log_2(1-q) + p(a_2b_2)log_2 q]. \end{aligned} \tag{43}$$

Note that the joint probability and conditional probability has relationship in (44).

$$\begin{aligned} p(a_i b_j) &= p(a_i)p(b_j|a_i) \\ &= p(b_j)p(a_i|b_j). \end{aligned} \tag{44}$$

Combining (43) and (44) together, (43) becomes:

$$\begin{aligned} H(Y|X) = -\,&[p_2(qlog_2 q + (1-q)log_2(1-q)) \\ &+ p_1(plog_2 p + (1-p)log_2(1-p))]. \end{aligned} \tag{45}$$

Next step is to find the information destination entropy $H(Y)$.

$$\begin{aligned} H(Y) &= -\sum_{j=1}^{2} p(b_j)log_2 p(b_j) \\ &= -[p(b_1)log_2 p(b_1) + p(b_2)log_2 p(b_2)]. \end{aligned} \tag{46}$$

To solve for (46), the marginal probability $p(b_j)$ is needed.

$$\begin{aligned} p(b_j) &= \sum_{i=1}^{2} p(a_i)p(b_j|a_i) \\ &= p(a_1b_j) + p(a_2b_j). \end{aligned} \tag{47}$$

Combining (46) and (47), (46) becomes

$$\begin{aligned} H(Y) = -\,&[(p_1 p + p_2(1-q))log_2(p_1 p + p_2(1-q)) \\ &+ (p_1(1-p) + p_2 q)log_2(p_1(1-p) + p_2 q)]. \end{aligned} \tag{48}$$

Therefore, (41) becomes

$$\begin{aligned} C &= maxI(Y;X) = max[H(Y) - H(Y|X)] \\ &= max[-(p_1 p + p_2(1-q))log_2(p_1 p + p_2(1-q)) \\ &\quad - (p_1(1-p) + p_2 q)log_2(p_1(1-p) + p_2 q) \\ &\quad + p_2(qlog_2 q + (1-q)log_2(1-q)) \\ &\quad + p_1(plog_2 p + (1-p)log_2(1-p))]. \end{aligned} \tag{49}$$

IV. Numerical Results

In this section, we will use molecule-based simulation to validate our proposed analytical MCN model employing the default parameters in Table. II. In addition, the BER and channel capacity performance are analyzed under conditions of different numbers of capillaries, time slot length, receiver size, decision threshold, inlet flow velocity and number of released molecules.

TABLE II: Simulation Parameters

Default Parameter	**Value**	**Unit**
Blood Viscosity	0.0035 [40]	$Pa \cdot s$
Blood Velocity	10 [40]	mm/s
Diffusion Coefficient	1300 [62]	$\mu m^2/s$
Arteriole length	800 [57]	μm
Arteriole Radius	35 [57]	μm
Number of Capillaries	100	-
Capillary Length	600-1200 [40]	μm
Capillary Radius	8-12 [40]	μm
Venule length	1500 [60]	μm
Venule Radius	53 [60]	μm
Time slot	5	s
receiver size ratio α	0.5	-
Released Molecules	10000	-

In Fig. 9, under the default parameters, the results obtained from particle simulation show that the received molecules and concentration curve of MCN through a single capillary are close to the derived mathematical model in (25)-(28). The simulation curve differs a little from the theoretical one, and this is because of the fluctuation caused by the delay of some molecules. Fig. 10 shows the CIR of MCN with different numbers of capillaries ranging from 10 to 300. It is worth noting that as the number of capillaries increases, the curve becomes less steep and the maximum amplitude decreases significantly. When the number is greater than 100, the curve becomes like

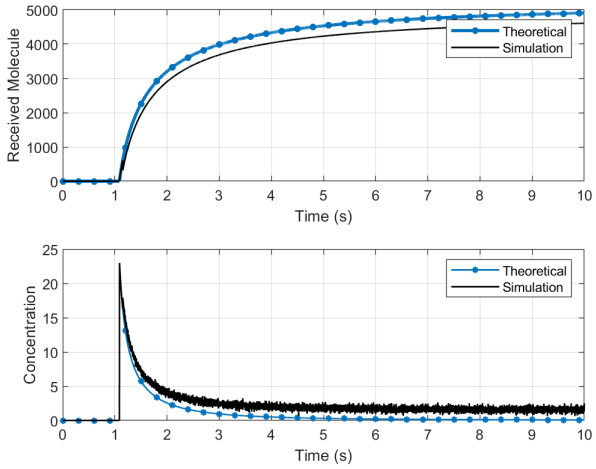

Fig. 9: Concentration of Received Molecules through a single capillary in MCN

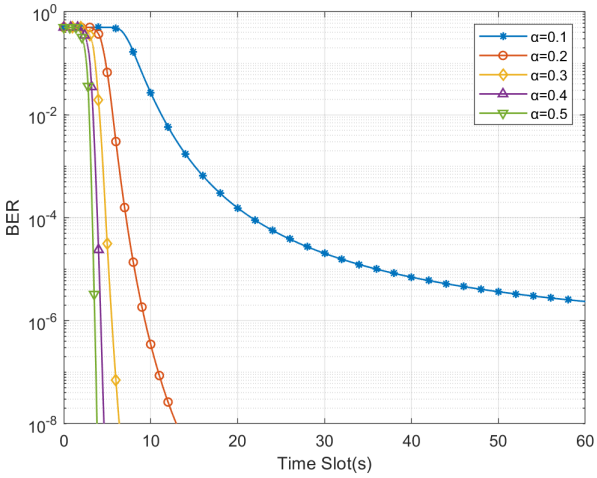

Fig. 11: BER verses Receiver Size

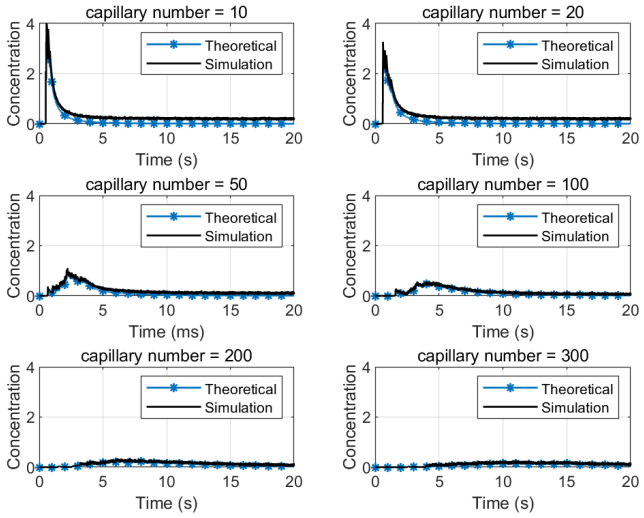

Fig. 10: CIR of MCN with different numbers of capillaries

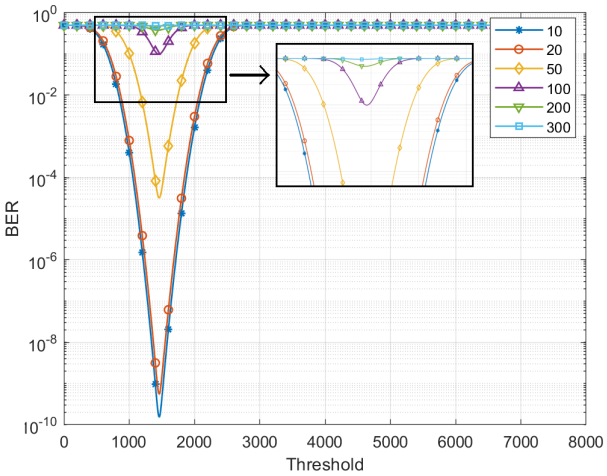

Fig. 12: BER verses decision threshold for different numbers of capillaries

a flat line, making the signal almost not detectable. This is because the number of released molecules is fixed, and as the number of capillaries increases, the information molecules are distributed in more capillaries, resulting in fewer information molecules in each capillary. In addition, since the length of capillaries varies, the time that molecule takes to pass through more capillaries will cause the time of arrival to spread over a large period of time, resulting in a very flat signal curve. To address this problem, the transmitter can send a larger number of molecules or simply increase the time slot length. We will show the results in the following figures.

Fig. 11 compared the impact of different sizes of receiver. The receiver is assumed to be passive and only molecules that pass through it are counted. A larger receiver means a stronger CIR signal. It shows that when the receiver size ratio α= 0.1, the BER is much higher than α= 0.2, and when α increases, the BER significantly decreases. It means the size of receiver can be a decisive factor in MCN communication channel. A larger receiver can help achieve a low BER with a shorter time slot length, which can improve its bit rate of the system.

In Fig. 12, we compared the BER of MCN with different number of capillaries. The released molecule number is 10000, and we set the threshold from 0 to 8000. We found out that the best threshold that helps achieve a minimum BER is the same as (37). The enlarged part in the figure shows that when the number of capillaries exceeds 100, the BER is already very poor, which means adjusting threshold is no longer enough to mitigate the BER.

Fig. 13 to Fig. 15 compared the impact of released molecule number N_{tx}, time slot length and inlet velocity on BER. Fig. 13 shows that increasing the number of molecules can to some extent improve the BER performance when capillary number is greater than 100. With the capillary number is 300, even when number of released molecules is 6×10^6, the BER is still very poor. However, Fig. 14 shows that increasing time slot length is very effective. By increasing time slot length to 15s, the BER performance is acceptable even when the capillary number is high. However, it takes the cost of bit

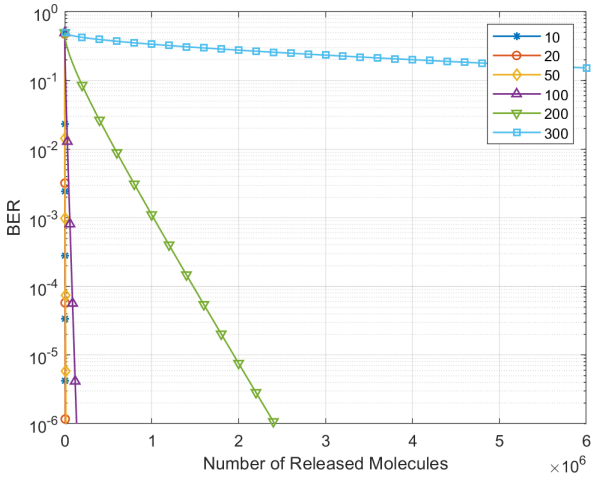

Fig. 13: BER verses Released Molecules for different numbers of capillaries

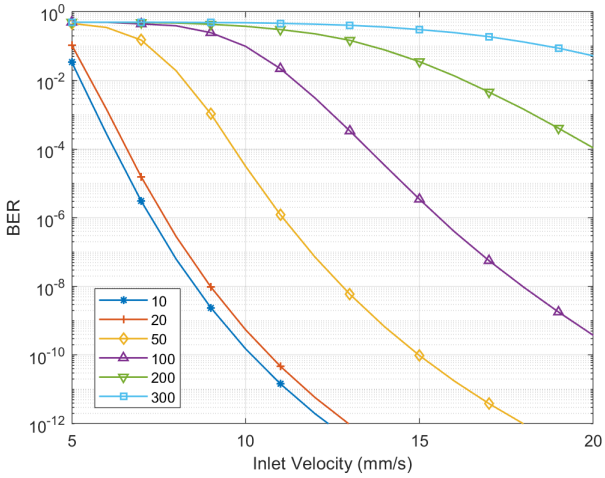

Fig. 15: BER verses inlet velocity for different numbers of capillaries

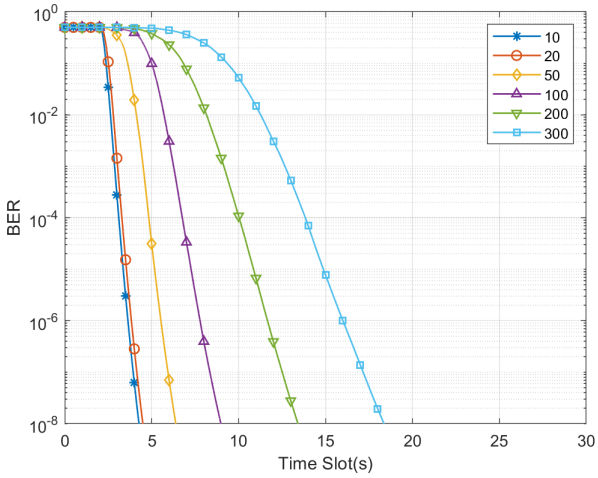

Fig. 14: BER verses Time slot for different numbers of capillaries

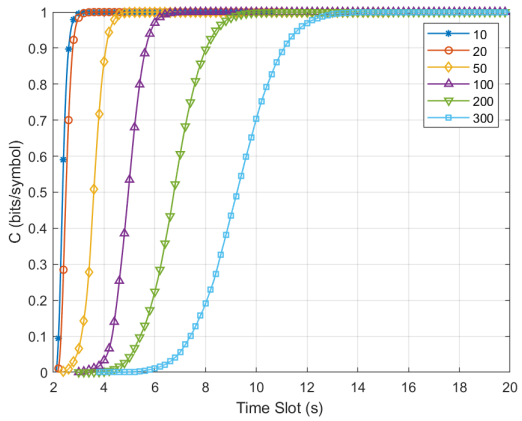

Fig. 16: Relationship of Channel Capacity and Time slot length with numbers of capillaries

rate. In different MCN, the inlet velocity may vary, however, it has a moderate impact on BER, shown in Fig. 15. When the inlet velocity is 20mm/s, the BER is still very poor when the capillary number is high.

However, the cost of efficiency can not be ignored. As time slot length continues to increase, the bit rate will first reach an apex and then drop after the channel capacity reaches its maximum as shown in Fig. 17.

In the channel capacity parts, we have analyzed the influence of different time slot lengths and receiver size. The results are similar to that of BER. Fig. 16 shows that when time slot length increases, the bit per symbol increase as well, which proves that a larger time slot length can help improve the communication in MCN with a high number of capillaries.

At last we compared the impact of receiver size α. In Fig.18, when α is 0.1, the capacity is nearly 5% of that when α is 0.4. It still shows that receiver size is a decisive factor in MCN system.

V. Conclusion

In this paper, we have analyzed the physical model of blood flow and micro-circulation and proposed a communication channel modeling based on it. We derived the channel impulse response of arteriole, capillary network and venule, respectively. We used both Bit error rate and channel capacity to evaluate its communication performance based on CSK modulation and summarized the factors that have the greatest impact on MCN communication.

It shows that the blood vessel channel has a much faster bit rate than that of a diffusion based channel and it enables the communication in the order of mm with a relatively high bit rate. In the micro-circulation, the main interference comes from massive capillary network. However the interference can be mitigated by increasing time slot length and released number of molecules. It can be concluded that MCN has the potential of supporting internet of things within human body with a moderate bit rate. In the future, we will consider design an effective coding and modulation method to combat the interference.

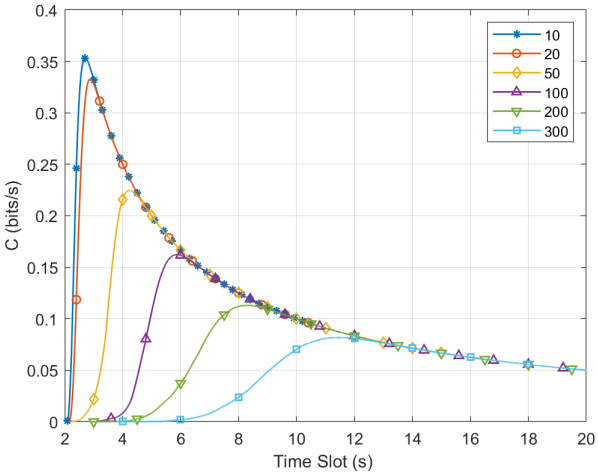

Fig. 17: Relationship of Bit Rate and and Time slot length with different numbers of capillaries

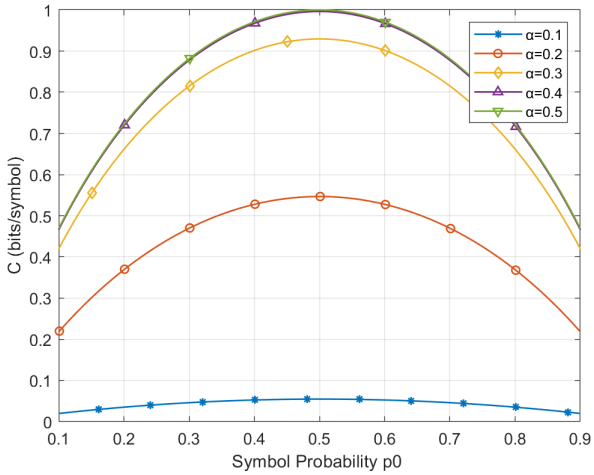

Fig. 18: Relationship of Channel Capacity and symbol probability with different Receiver Size

REFERENCES

[1] I. F. Akyildiz, M. Pierobon, S. Balasubramaniam and Y. Koucheryavy, "The internet of Bio-Nano things," in IEEE Communications Magazine, vol. 53, no. 3, pp. 32-40, March 2015, doi: 10.1109/MCOM.2015.7060516.

[2] Bock, Sander De et al. Our capricious vessels: The influence of stent design and vessel geometry on the mechanics of intracranial aneurysm stent deployment. *Journal of biomechanics* 45 8 (2012): 1353-9 .

[3] Qiuhua, Zou et al. Mechanical characteristics of novel polyester/NiTi wires braided composite stent for the medical application. *Results in physics* 6 (2016): 440-446.

[4] Adams, David H. et al. Transcatheter aortic-valve replacement with a self-expanding prosthesis. *The New England journal of medicine* 370 19 (2014): 1790-8 .

[5] García, A. et al. Influence of geometrical parameters on radial force during self-expanding stent deployment. Application for a variable radial stiffness stent. *Journal of the mechanical behavior of biomedical materials* 10 (2012): 166-75 .

[6] Y. Sun, M. Liu, Y. Xiao, and Y. Chen, A novel molecular communication inspired detection method for the evolution of atherosclerosis, Computer Methods and Programs in Biomedicine, vol. 219, p. 106756, Jun. 2022, doi: 10.1016/j.cmpb.2022.106756.

[7] M. Mimee et al."An ingestible bacterial-electronic system to monitor gastrointestinal health." *Science360*,915-918(2018).DOI:10.1126/science.aas9315

[8] P. Nadeau, M. Mimee, S. Carim, T. K. Lu and A. P. Chandrakasan, "21.1 Nanowatt circuit interface to whole-cell bacterial sensors," 2017 IEEE International Solid-State Circuits Conference (ISSCC), San Francisco, CA, USA, 2017, pp. 352-353, doi: 10.1109/ISSCC.2017.7870406.

[9] Danino, T., Mondragón-Palomino, O., Tsimring, L. et al. A synchronized quorum of genetic clocks. Nature 463, 326330 (2010). https://doi.org/10.1038/nature08753

[10] Jonas, Oliver et al. An implantable microdevice to perform high-throughput in vivo drug sensitivity testing in tumors. Science translational medicine vol. 7,284 (2015): 284ra57. doi:10.1126/scitranslmed.3010564

[11] Samiei, Ehsan et al. A review of digital microfluidics as portable platforms for lab-on a-chip applications. Lab on a chip vol. 16,13 (2016): 2376-96. doi:10.1039/c6lc00387g

[12] Dahlman, James E et al. Barcoded nanoparticles for high throughput in vivo discovery of targeted therapeutics. Proceedings of the National Academy of Sciences of the United States of America vol. 114,8 (2017): 2060-2065. doi:10.1073/pnas.1620874114

[13] Shi, Huanhuan et al. Recent progress of microfluidic reactors for biomedical applications. Chemical Engineering Journal (2019): n. pag.

[14] J. S. McLean, "A re-examination of the fundamental limits on the radiation Q of electrically small antennas," in IEEE Transactions on Antennas and Propagation, vol. 44, no. 5, pp. 672-, May 1996, doi: 10.1109/8.496253.

[15] D. F. Sievenpiper et al., "Experimental Validation of Performance Limits and Design Guidelines for Small Antennas," in IEEE Transactions on Antennas and Propagation, vol. 60, no. 1, pp. 8-19, Jan. 2012, doi: 10.1109/TAP.2011.2167938.

[16] I. F. Akyildiz, F. Brunetti, C. Blazquez, Nanonetworks: A new communication paradigm, *Computer Networks (Elsevier) Journal* 52 (12) (2008) 22602279.

[17] N. Farsad, H. Yilmaz, A. Eckford, C. Chae and W. Guo, "A comprehensive survey of recent advancements in molecular communication," *IEEE Commun. Surveys Tuts.*, vol. 18, no. 3, pp. 18871919, 3rd Quart., 2014.

[18] I. F. Akyildiz, M. Pierobon, S. Balasubramaniam, and Y. Koucheryavy, "Internet of BioNanoThings," *IEEE Commun. Mag.*, vol. 53, no. 3, pp. 3240, Mar. 2015.

[19] T. Nakano, A. Eckford, and T. Haraguchi, *Molecular Communication*. Cambridge University Press, 2013.

[20] T. Suda, M. J. Moore, T. Nakano, "Exploratory research on molecular communication between nanomachines," *Nature Computing*, pp. 130, 2005.

[21] T. Nakano, T. Suda, Y. Okaie, M. J. Moore and A. V. Vasilakos, "Molecular Communication Among Biological Nanomachines: A Layered Architecture and Research Issues," in *IEEE Transactions on NanoBioscience*, vol. 13, no. 3, pp. 169-197, Sept. 2014, doi: 10.1109/TNB.2014.2316674.

[22] B. Krishnaswamy et al., "Time-Elapse Communication: Bacterial Communication on a Microfluidic Chip," in *IEEE Transactions on Communications*, vol. 61, no. 12, pp. 5139-5151, December 2013, doi: 10.1109/TCOMM.2013.111013.130314.

[23] M. S. Kuran, H. B. Yilmaz, T. Tugcu and I. F. Akyildiz, "Modulation Techniques for Communication via Diffusion in Nanonetworks," *2011 IEEE International Conference on Communications (ICC)*, Kyoto, Japan, 2011, pp. 1-5, doi: 10.1109/icc.2011.5962989.

[24] M. J. Moore, T. Suda and K. Oiwa, "Molecular Communication: Modeling Noise Effects on Information Rate," in *IEEE Transactions on NanoBioscience*, vol. 8, no. 2, pp. 169-180, June 2009, doi: 10.1109/TNB.2009.2025039.

[25] H. Arjmandi, A. Gohari, M. N. Kenari and F. Bateni, "Diffusion-Based Nanonetworking: A New Modulation Technique and Performance Analysis," in *IEEE Communications Letters*, vol. 17, no. 4, pp. 645-648, April 2013, doi: 10.1109/LCOMM.2013.021913.122402.

[26] B. Atakan, S. Galmes and O. B. Akan, "Nanoscale Communication With Molecular Arrays in Nanonetworks," in *IEEE Transactions on NanoBioscience*, vol. 11, no. 2, pp. 149-160, June 2012, doi: 10.1109/TNB.2011.2181862.

[27] N. Garralda et al. "Diffusion-based physical channel identification in molecular nanonetworks." *NanoCommunication Networks* 2.4 (2011): 196-204.

[28] P. -C. Yeh et al., "A new frontier of wireless communication theory: diffusion-based molecular communications," in *IEEE Wireless Communications*, vol. 19, no. 5, pp. 28-35, Oct. 2012, doi: 10.1109/MWC.2012.6339469.

[29] T. Nakano, M. J. Moore, W. Fang, "Molecular communication and networking: Opportunities and challenges," in *IEEE Transactions on NanoBioscience*. vol.11, pp. 135148, May 2012.

[30] J. Wang, S. Öüt, H. Al Hassanieh, and B. Krishnaswamy, Towards Practical and Scalable Molecular Networks, in Proceedings of the ACM SIGCOMM 2023 Conference, New York NY USA: ACM, Sep. 2023, pp. 6276. doi: 10.1145/3603269.3604881.

[31] A. Einolghozati, M. Sardari, and F. Fekri, "Capacity of diffusion-based molecular communication with ligand receptors," in *2011 IEEE Information Theory Workshop*, Paraty, Brazil: IEEE, Oct. 2011, pp. 8589. doi: 10.1109/ITW.2011.6089591.

[32] V. Jamali, A. Ahmadzadeh, W. Wicke, A. Noel, and R. Schober, Channel Modeling for Diffusive Molecular CommunicationA Tutorial Review, Proc. IEEE, vol. 107, no. 7, pp. 12561301, Jul. 2019, doi: 10.1109/JPROC.2019.2919455.

[33] X. Bao, Y. Zhu, and W. Zhang, "Channel Characteristics for Molecular Communication via Diffusion With a Spherical Boundary," *IEEE Wireless Commun. Lett.*, vol. 8, no. 3, pp. 957960, Jun. 2019, doi: 10.1109/LWC.2019.2902093.

[34] H. Arjmandi, M. Movahednasab, A. Gohari, M. Mirmohseni, M. Nasiri-Kenari and F. Fekri, "ISI-Avoiding Modulation for Diffusion-Based Molecular Communication," in *IEEE Transactions on Molecular, Biological and Multi-Scale Communications*, vol. 3, no. 1, pp. 48-59, March 2017, doi: 10.1109/TMBMC.2016.2640311.

[35] B. Tepekule, A. E. Pusane, H. B. Yilmaz and T. Tugcu, "Energy efficient ISI mitigation for communication via diffusion," *2014 IEEE International Black Sea Conference on Communications and Networking (BlackSeaCom)*, Odessa, Ukraine, 2014, pp. 33-37, doi: 10.1109/BlackSeaCom.2014.6848999.

[36] A. Noel and D. Makrakis, Algorithm for Mesoscopic AdvectionDiffusion, IEEE Trans.on Nanobioscience, vol. 17, no. 4, pp. 543554, Oct. 2018, doi: 10.1109/TNB.2018.2878065.

[37] W. Wicke, T. Schwering, A. Ahmadzadeh, V. Jamali, A. Noel, and R. Schober, "Modeling Duct Flow for Molecular Communication," in 2018 IEEE Global Communications Conference (GLOBECOM), Abu Dhabi, United Arab Emirates: IEEE, Dec. 2018, pp. 206212. doi: 10.1109/GLOCOM.2018.8647632.

[38] L. Felicetti, M. Femminella, and G. Reali, "Simulation of molecular signaling in blood vessels: Software design and application to atherogenesis," Nano Communication Networks, vol. 4, no. 3, pp. 98119, Sep. 2013, doi: 10.1016/j.nancom.2013.06.002.

[39] Tuma R.F., W.N. Duran, and K. Ley, *Microcirculation*. San Diego Academic Press, 2008.

[40] Bessonov, Nikolay, et al. "Methods of blood flow modelling." Mathematical modelling of natural phenomena 11.1 (2016): 1-25.

[41] L. Back, J. Radbill, Y. Cho, and D. Crawford, "Measurement and prediction of flow through a replica segment of a mildly atherosclerotic coronary artery of man," J. Biomech.,vol.19, no. 1, pp. 117, 1986.

[42] J. A. Jensen, "Lectures Notes on Medical Imaging SystemsLecture 5: Blood Flow in the Human Body." Lyngby, Denmark: Technical Univ. of Denmark, 2018.

[43] Funck, Carsten et al. Characterization of the diffusion coefficient of blood. Magnetic resonance in medicine vol. 79,5 (2018): 2752-2758. doi:10.1002/mrm.26919

[44] Ye, Fei et al. In-vivo full-field measurement of microcirculatory blood flow velocity based on intelligent object identification. Journal of biomedical optics vol. 25,1 (2020): 1-11. doi:10.1117/1.JBO.25.1.016003

[45] Jayalalitha, G et al. Fractal model for blood flow in cardiovascular system. Computers in biology and medicine vol. 38,6 (2008): 684-93. doi:10.1016/j.compbiomed.2008.03.002

[46] Leary, Scott P et al. Toward the emergence of nanoneurosurgery: part III–nanomedicine: targeted nanotherapy, nanosurgery, and progress toward the realization of nanoneurosurgery. Neurosurgery vol. 58,6 (2006): 1009-26; discussion 1009-26. doi:10.1227/01.NEU.0000217016.79256.16

[47] Couvreur, Patrick, and Christine Vauthier. Nanotechnology: intelligent design to treat complex disease. Pharmaceutical research vol. 23,7 (2006): 1417-50. doi:10.1007/s11095-006-0284-8

[48] Patel, Geeta M et al. Nanorobot: a versatile tool in nanomedicine. Journal of drug targeting vol. 14,2 (2006): 63-7. doi:10.1080/10611860600612862

[49] Femminella, Mauro et al. A Molecular Communications Model for Drug Delivery. IEEE transactions on nanobioscience vol. 14,8 (2015): 935-45. doi:10.1109/TNB.2015.2489565

[50] Chude-Okonkwo, Uche A K et al. Molecular Communication Model for Targeted Drug Delivery in Multiple Disease Sites With Diversely Expressed Enzymes. IEEE transactions on nanobioscience vol. 15,3 (2016): 230-45. doi:10.1109/TNB.2016.2526783

[51] Chahibi, Youssef et al. Molecular Communication Modeling of Antibody-Mediated Drug Delivery Systems. IEEE transactions on bio-medical engineering vol. 62,7 (2015): 1683-95. doi:10.1109/TBME.2015.2400631

[52] U. A. K. Chude-Okonkwo, "Diffusion-controlled enzyme-catalyzed molecular communication system for targeted drug delivery," 2014 IEEE Global Communications Conference, Austin, TX, USA, 2014, pp. 2826-2831, doi: 10.1109/GLOCOM.2014.7037236.

[53] Y. Chahibi, M. Pierobon, S. O. Song, and I. F. Akyildiz, A Molecular Communication System Model for Particulate Drug Delivery Systems, IEEE Trans. Biomed. Eng., vol. 60, no. 12, pp. 34683483, Dec. 2013, doi: 10.1109/TBME.2013.2271503.

[54] B. Atakan, O. B. Akan and S. Balasubramaniam, "Body area nanonetworks with molecular communications in nanomedicine," in IEEE Communications Magazine, vol. 50, no. 1, pp. 28-34, January 2012, doi: 10.1109/MCOM.2012.6122529.

[55] Fagrell, B, and M Intaglietta. "Microcirculation: its significance in clinical and molecular medicine." Journal of internal medicine vol. 241,5 (1997): 349-62. doi:10.1046/j.1365-2796.1997.125148000.x

[56] Joyner, W L et al. "Intravascular pressure distribution and dimensional analysis of microvessels in hamsters with renovascular hypertension." Microvascular research vol. 22,2 (1981): 190-8. doi:10.1016/0026-2862(81)90088-1

[57] Kuo, L et al. "Myogenic activity in isolated subepicardial and subendocardial coronary arterioles." The American journal of physiology vol. 255,6 Pt 2 (1988): H1558-62. doi:10.1152/ajpheart.1988.255.6.H1558

[58] Bassingthwaighte, J B et al. Microvasculature of the dog left ventricular myocardium. Microvascular research vol. 7,2 (1974): 229-49. doi:10.1016/0026-2862(74)90008-9

[59] Ley, K et al. "Topological structure of rat mesenteric microvessel networks." Microvascular research vol. 32,3 (1986): 315-32. doi:10.1016/0026-2862(86)90068-3

[60] House, S D, and P C Johnson. "Diameter and blood flow of skeletal muscle venules during local flow regulation." The American journal of physiology vol. 250,5 Pt 2 (1986): H828-37. doi:10.1152/ajpheart.1986.250.5.H828

[61] R. Mosayebi, A. Ahmadzadeh, W. Wicke, V. Jamali, R. Schober, and M. Nasiri-Kenari, "Early Cancer Detection in Blood Vessels Using Mobile Nanosensors," IEEE Trans.on Nanobioscience, vol. 18, no. 2, pp. 103116, Apr. 2019, doi: 10.1109/TNB.2018.2885463.

[62] M. S. Kuran, H. B. Yilmaz, T. Tugcu, and B. Ozerman, "Energy model for communication via diffusion in nanonetworks," *Nano Communication Networks*, vol. 1, no. 2, pp. 8695, 2010.

[63] M. S. Leeson and M. D. Higgins, "Forward error correction for molecular communications," *Nano Communication Networks*, vol. 3, no. 1, pp. 161167, 2012

[64] A. Noel, K. C. Cheung and R. Schober, "Improving Receiver Performance of Diffusive Molecular Communication With Enzymes," in *IEEE Transactions on NanoBioscience*, vol. 13, no. 1, pp. 31-43, March 2014, doi: 10.1109/TNB.2013.2295546.

[65] C. Jiang, Y. Chen and K. J. R. Liu, "Inter-user interference in molecular communication networks," *2014 IEEE International Conference on Acoustics, Speech and Signal Processing (ICASSP)*, Florence, Italy, 2014, pp. 5725-5729, doi: 10.1109/ICASSP.2014.6854700.

[66] Q. Liu, Z. Lu and K. Yang, "Modeling and Dual Threshold Algorithm for Diffusion-Based Molecular MIMO Communications," in *IEEE Transactions on NanoBioscience*, vol. 20, no. 4, pp. 416-425, Oct. 2021, doi: 10.1109/TNB.2021.3077297.

[67] M. Pierobon and I. F. Akyildiz, "Intersymbol and co-channel interference in diffusion-based molecular communication," *2012 IEEE International Conference on Communications (ICC)*, Ottawa, ON, Canada, 2012, pp. 6126-6131, doi: 10.1109/ICC.2012.6364970.

[68] M. S. Kuran, H. B. Yilmaz, T. Tugcu, and I. F. Akyildiz, "Interference effects on modulation techniques in diffusion based nanonetworks," *NanoCommunication Networks*, vol. 3, no. 1, pp. 6573, 2012.